Moldable AR microstructures for improved laser transmission and damage resistance in CIRCM fiber optic beam delivery systems

Bruce D. MacLeod*, Douglas S. Hobbs, and Ernest Sabatino III
TelAztec LLC, 15 A Street, Burlington, MA, USA 01803-3404

ABSTRACT

Anti-reflecting (AR) surface relief microstructures (ARMs) are being developed as a replacement for thin-film AR coatings in laser-based systems to improve light transmission, power handling, operational bandwidth, and system reliability. Because ARMs textures have the potential to be replicated using simple embossing methods, the performance advantage and robustness of ARMs can be extended to moldable mid-infrared transmitting materials such as chalcogenide optical fibers. In this work, the optical performance of mid-infrared transparencies incorporating ARMs textures replicated from a master template has been modeled, and multiple master stamping tools have been fabricated in materials such as diamond, silicon carbide, nickel, silicon, and sapphire. Images from ARMs texture embossing trials using arsenic sulfide and arsenic selenide (AMTIR2) glasses, and fluoride glasses such as ZBLAN and indium fluoride provided by IRPhotonics, show excellent pattern transfer and fidelity. Transmission measurements of ARMs textures stamped into arsenic sulfide and arsenic selenide windows show broadband infrared performance equivalent to ARMs textured windows processed by direct patterning and etch methods. A system for molding ARMs textures directly into the end facets of multi-mode mid-infrared transmitting fibers is yielding promising initial results.

Keywords: Chalcogenide, Antireflection, Motheye, Laser damage, Mid-IR Fiber, CIRCM, IRCM, High power lasers

1. INTRODUCTION

Potential Common Infrared Counter Measure (CIRCM) systems utilize high power lasers to actively blind or confuse the targeting and tracking sensors on board a missile threat[1-3]. CIRCM system designs may benefit from a new class of optical fibers based on chalcogenide and fluoride glass materials that can allow for the efficient distribution of a high power infrared laser source to multiple jamming turrets around a military or commercial aircraft[4-5]. These glasses are moldable at low temperatures and pressures enabling the inexpensive fabrication of other CIRCM optical components such as refractive and diffractive lenses[6-7], windows, filters[8], and prisms. Because of the high optical power in CIRCM systems, some form of antireflection (AR) treatment is needed to maximize transmission and avoid potentially damaging or de-stabilizing reflections. Multiple-layer thin-film AR coatings are expensive and impractical for fiber delivery systems, exhibiting low laser damage resistance that limits the laser power transmission capacity to the point where CIRCM mission objectives cannot be met. An alternative, microstructure-based AR treatment that can be inexpensively molded in the end facets of chalcogenide and fluoride fibers, has been shown to be capable of high transmission combined with increased laser damage resistance[11,12]. A scanning electron microscope (SEM) image of AR microstructures, or ARMs, embossed in the tip of an arsenic-selenide-tellurium (As_2Se_3 with Te) fiber provided by Amorphous Materials Inc. of Garland Texas, is shown here on the right. The goal of this work is to demonstrate an initial capability to generate master templates and to directly replicate AR microstructures in the arsenic sulfide (As_2S_3) and As_2Se_3 fibers being commercialized by CorActive High-Tech Inc. of Canada and IRFlex Corp. of Danville Virginia, as well as the indium fluoride (InF_3) and ZBLAN fibers being commercialized by IRPhotonics of Hamden Connecticut.

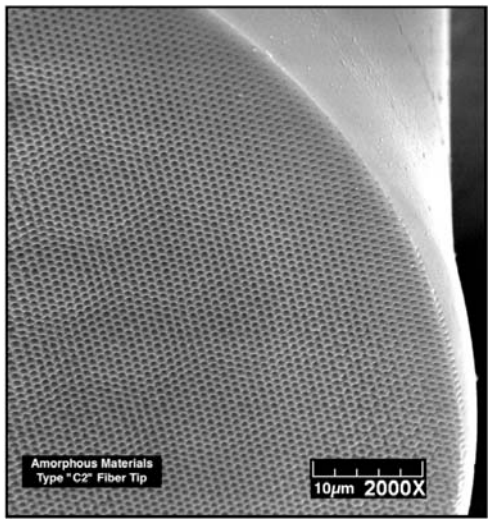

In prior demonstrations, both the Naval Research Laboratories (NRL) and BAE Systems Inc. have utilized thin nickel master plates designed and produced by TelAztec to emboss AR microstructures in the end facets of As2S3 fibers. The SEM images on the left side of Figure 1 show an array of tapered holes on a square grid with an 800nm spacing

* bdmacleod@telaztec.com; phone 1 781 229-9905; fax 1 781 229-2195; www.telaztec.com

embossed by NRL where the core and cladding of the fiber are indicated and a magnified elevation view of the AR microstructures is given as an inset. NRL has reported a broad-band mid-infrared (mid-IR) transmission increase of over 10% for a single fiber facet embossed with ARMs[5], and most notably have recorded a continuous wave laser power transmission capacity of over one gigawatt per square centimeter (1GW/cm^2), a level about five times higher than the typical threshold for damage found with thin-film AR coated fibers[9]. Fiber tips embossed by BAE with ARMs textures such as the hexagonal array of post structures on an 800nm grid shown on the right side of Figure 1 – have exhibited a nearly theoretical maximum transmission increase of 15% over the entire mid-IR spectral band[9].

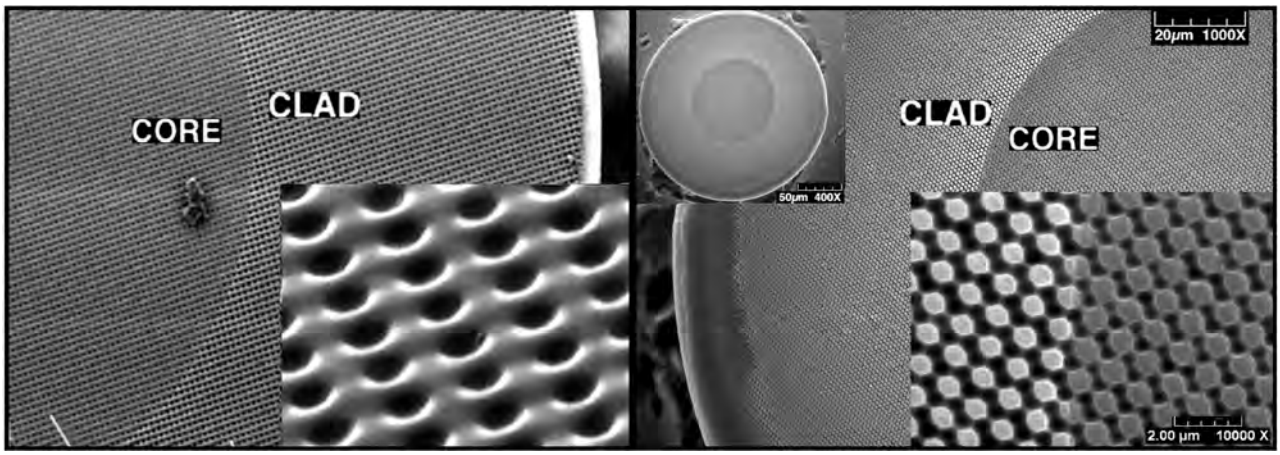

Figure 1: SEM images of ARMs textures embossed in As_2S_3 fiber facets by NRL (left) and BAE (right). Magnified images showing the ARMs detail are inset in the lower right corner of each frame.

2. THIN-FILM ANTI-REFLECTION TECHNOLOGY

The application a broadband AR coating on the 200-400µm diameter end facets of optical fibers requires the use of vacuum chambers that are not well suited for handling long fiber lengths. Only a small number of fibers can be coated at once, resulting in an expensive and inconsistent process. In addition, these fibers cannot be heated to optimal deposition temperatures, resulting in film adhesion and reproducibility issues. More significantly, during operation in mid-IR laser systems, thin film AR coating materials continue to exhibit unacceptable absorption leading to catastrophic, permanent damage to the fiber tips at power levels well below the requirements of CIRCM system applications. The SEM image in Figure 2 on the right shows a damage site in the top layer of a multi-layer thin-film AR coating deposited on a gallium arsenide (GaAs) substrate and designed for dual-band mid-IR operation, created during standardized laser damage testing at a wavelength of 2.1µm.

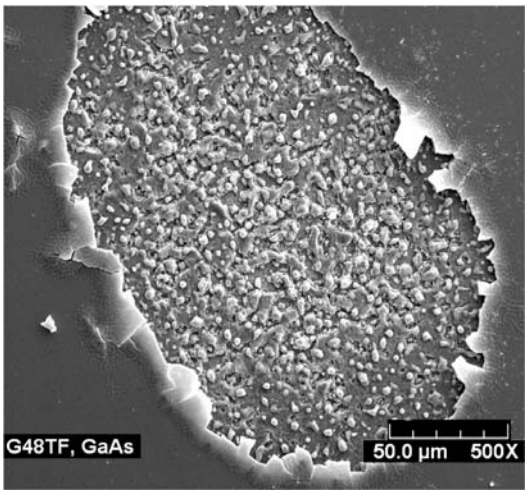

Figure 2: Overhead SEM image of a laser induced damage site in a thin-film AR coating on GaAs.

3. RECENT AR MICROSTRUCTURE PERFORMANCE DATA

Arrays of cone-type ARMs textures (often referred to as Motheye in the literature[13-23]) have been directly etched in the surface of 1-inch round, 2mm thick As_2S_3 windows supplied by NRL. The measured reflection of these windows before and after texturing with ARMs is given in Figure 3, where a mirror-based jig was utilized in a Thermo Nicolet FTIR spectrometer to record the spectral reflectance of mid-IR light incident ten degrees off the window surface normal. For such IR transparent plane parallel windows, isolating the front surface reflection is a challenge and was ultimately accomplished by roughening the back surface to produce diffuse scattered light that is less likely to be detected. This method may not have been completely effective – leading to a measured untreated surface reflection (solid black curve) 1% higher than expected from the established material properties. With this measurement error in mind, the spectral reflectance of an ARMs treated surface (solid grey curve) is reduced to the level of the FTIR noise

floor (dashed black curve) over the wavelength range of 1.8μm to 3.0μm, rising to an average of about 1% over the 3.5μm to 4.5μm range. A photograph of untreated (polished) and ARMs treated As_2S_3 windows together with a BAE fiber termination is given in the lower left corner of the plot. Also inset in the figure are elevation (left) and overhead (right) view SEM images detailing a fabricated ARMs texture consisting of a honeycomb array of cone structures nearly 2μm high with a grid spacing of 0.74μm.

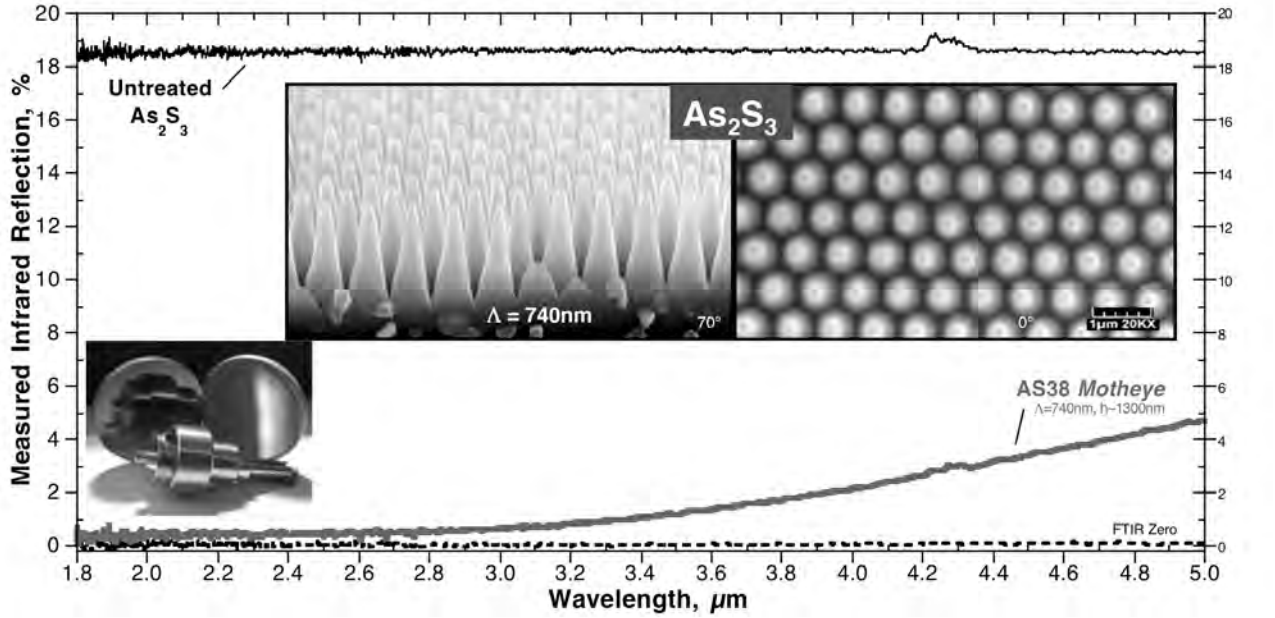

Figure 3: Measured reflection of untreated and ARMs-treated As_2S_3 windows along with SEM images detailing the texture.

To illustrate the laser damage resistance of ARMs textures, other mid-IR transmitting materials that may be used in CIRCM systems, were processed with ARMs textures designed for maximum transmission at a wavelength of 2μm. BAE provided several of their zinc germanium phosphide ($ZnGeP_2$, or ZGP) crystals that are capable of generating wavelength agile mid-IR laser energy[24,25] when illuminated by 2μm light. These 6x6mm, 14mm long crystals, one of which is shown on the right after the application of an ARMs texture in the entrance facet, were diced and polished into slabs to yield multiple test coupons. In addition to processing ARMs, several ZGP windows were coated with a multiple-layer thin-film AR stack designed for dual band mid-IR performance and deposited by Quality Thin Films, Inc. of Oldsmar Florida (QTF). Figure 4 is a plot comparing the transmission of mid-IR light through ZGP windows with no AR treatment (solid black line), to ZGP windows with ARMs textures in one surface (solid gray line), and ZGP windows with the QTF thin-film stack on one surface (dashed black curve). Overhead and elevation view SEMs showing the 0.61μm pitch honeycomb array of 0.7μm high cones that make up the Motheye-type ARMs texture in ZGP, are inset on the left side of the figure. As designed, the peak transmission for the ARMs treated samples occurs near the damage test laser wavelength of 2.09μm (marked by the vertical grey bar). While the ARMs treated sample performs better than the thin film coating at short wavelengths, the performance degrades at longer wavelengths due to the inadequate height of the cone structures. Process refinement is needed to obtain the full band performance comparable to the broadband As_2S_3 data shown in Figure 3.

Because GaAs is another transparent material that is useful for mid-IR windows and optics, and as a wavelength conversion device in a "periodically-poled" configuration, ARMs textures were also fabricated in GaAs wafers. In addition, GaAs has a refractive index that is a close match to ZGP, and could therefore be coated with the same thin-film AR stack to effect dual band mid-IR transmission. The mid-IR transmission of untreated, ARMs-treated, and thin film coated optical grade GaAs wafers was found to be nearly identical to the transmission data for ZGP windows shown in Figure 4. Figure 5 shows SEM images of the ARMs textures built in GaAs where again the cone height would need to be increased to obtain higher transmission over the longer wavelengths.

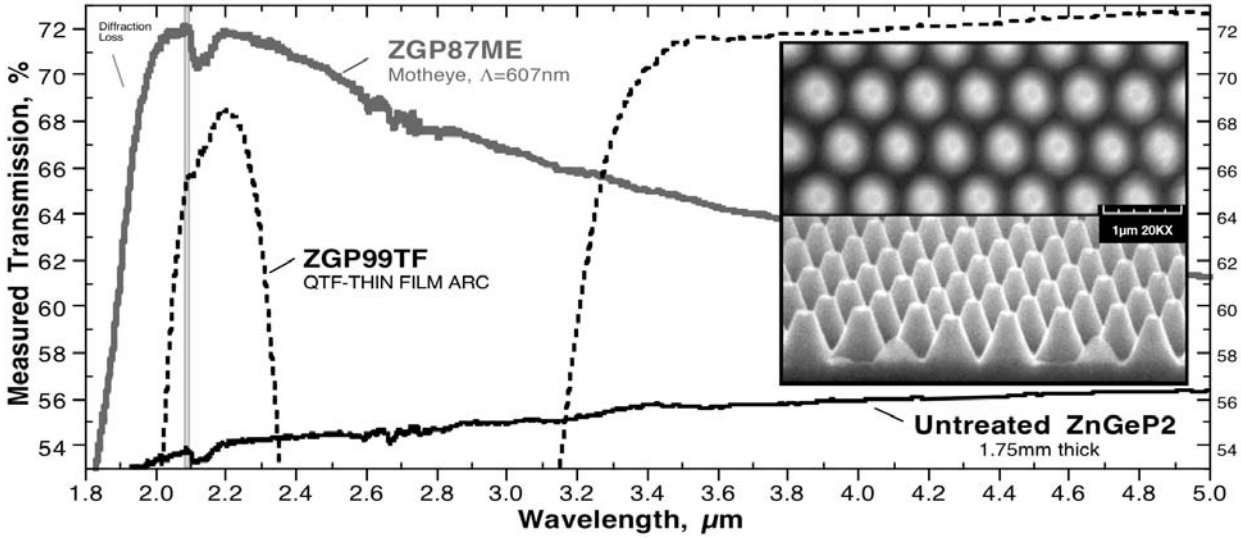

Figure 4: Measured transmission of mid-IR light through ARMs treated and thin film coated $ZnGeP_2$ windows.

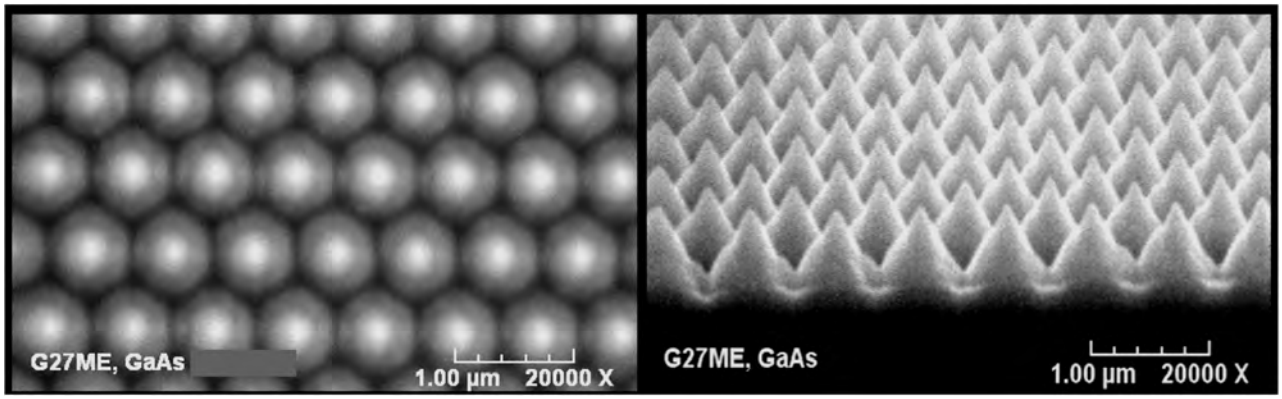

Figure 5: Overhead (left) and elevation (right) views of Motheye-type ARMs textures fabricated in a GaAs wafer.

To make a direct comparison of laser damage resistance of untreated, ARMs-treated, and thin-film AR coated windows, the As_2S_3, ZGP, and GaAs windows were subjected to short pulse duration 2.09μm wavelength laser induced damage threshold (LiDT) testing provided as a service by SPICA Technologies of New Hampshire. SPICA conducted standardized "S-on-1" tests with the laser system configured to deliver 80ns duration pulses at a 2Hz repetition rate and a spot size between 650 and 800μm, 100 pulses each location, with 10 energy levels. A plot of the damage frequency as a function of laser fluence level is given for the ZGP samples in Figure 6, where the data for two untreated ZGP windows is represented by the filled and open crosses and the solid black line, the data for two ARMs treated ZGP windows is represented by the filled and open triangles and the solid gray line, and the data for two thin-film AR coated ZGP windows is represented by the filled and open squares and the dashed black line. The data shows a threshold for damage of the ARMs treated ZGP windows that is about 75% of the damage threshold for untreated windows – but more than three times higher than the thin-film AR coated ZGP windows. A nearly identical result is found with the GaAs windows where the damage threshold of the ARMs-treated samples was 3.5 times higher than the thin film AR coated samples.

Figure 7 summarizes and compares the short pulse damage testing results at the 2μm wavelength for the three materials described above and cadmium zinc telluride (CdZnTe), a substrate used for infrared sensor arrays. As previously reported[28] the damage threshold for both the CdZnTe and As_2S_3 ARMs-treated windows was found to be 25% and 35% higher respectively than their untreated counterparts – a significant result that could advance the power transmission in CIRCM systems.

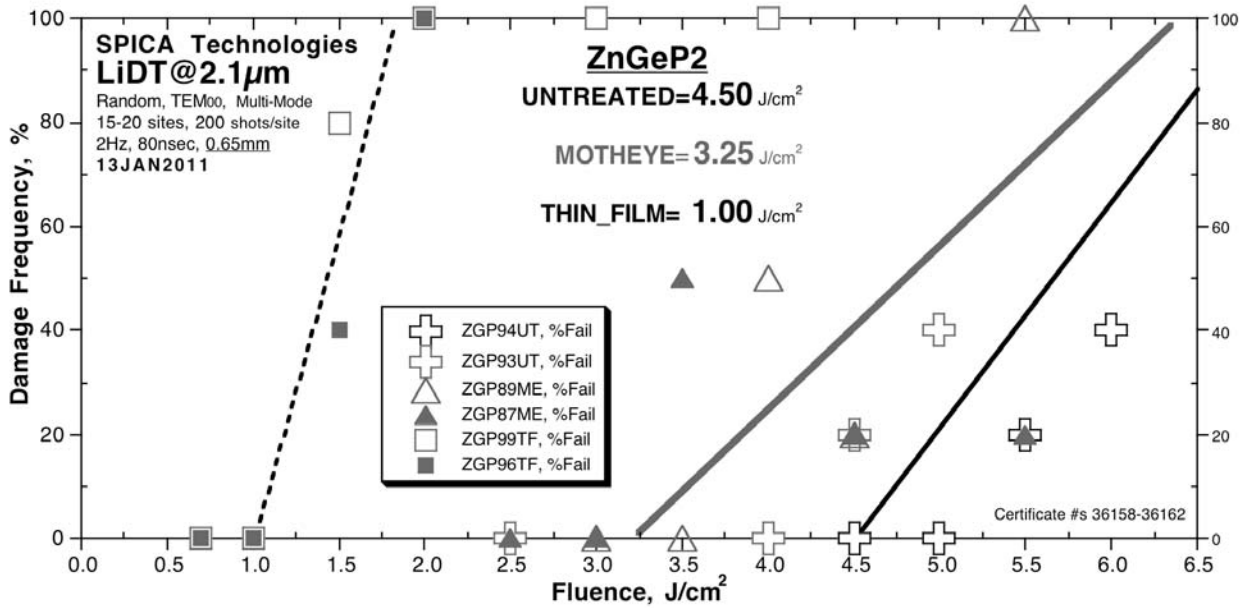

Figure 6: Damage frequency vs. pulsed laser fluence for untreated, ARMs-treated, and thin-film coated $ZnGeP_2$ windows.

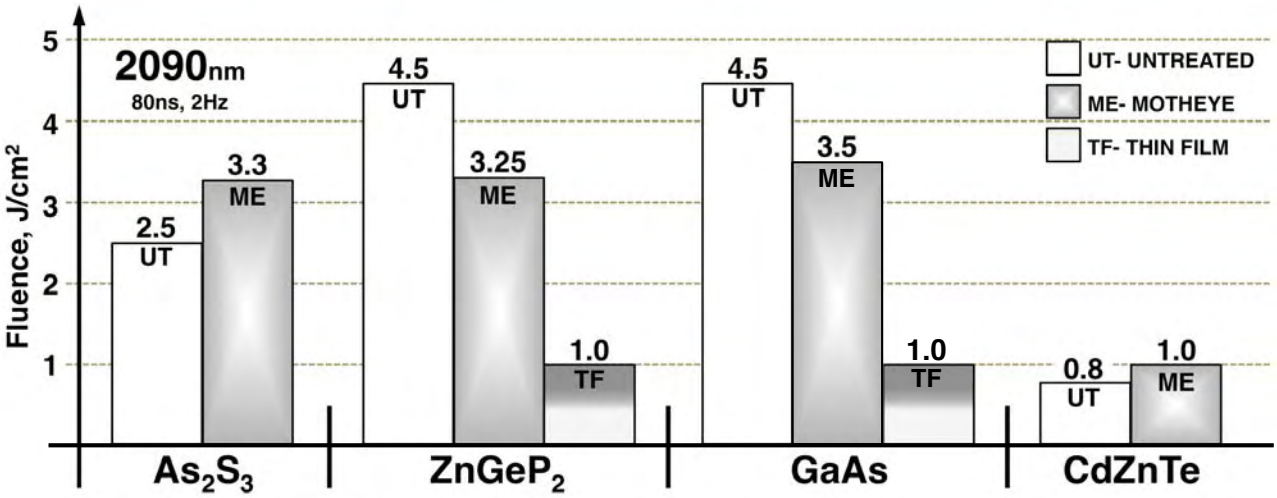

Figure 7: Summary of 2090nm pulsed LiDT tests of four mid-IR transmitting materials with various AR treatments.

4. ARMs PERFORMANCE THEORETICAL MODELING

TelAztec uses computer models to design and optimize the performance of ARMs textures. Using a rigorous vector diffraction calculation, the software predicts the spectral reflectance and transmittance of infrared light through a user defined three-dimensional surface texture. Typical simulation results as plotted in Figure 8, show the predicted performance of three types of ARMs textures- Motheye, Hybrid, and SWS, each with a periodicity of 800nm, embossed into the surface of an As_2S_3 window or fiber optic termination. The model indicates that both Motheye (solid black curve) and Hybrid (dashed black curve) ARMs can deliver broadband transmission efficiency, gaining an average of 15-17% over an untreated surface for both the shortwave pump and a broad range of lasing wavelengths. SWS ARMs can deliver almost 100% transmission within a narrower wavelength range, in this case at a lasing wavelength near 4.5μm, but cannot cover the full wavelength range of the CIRCM application.

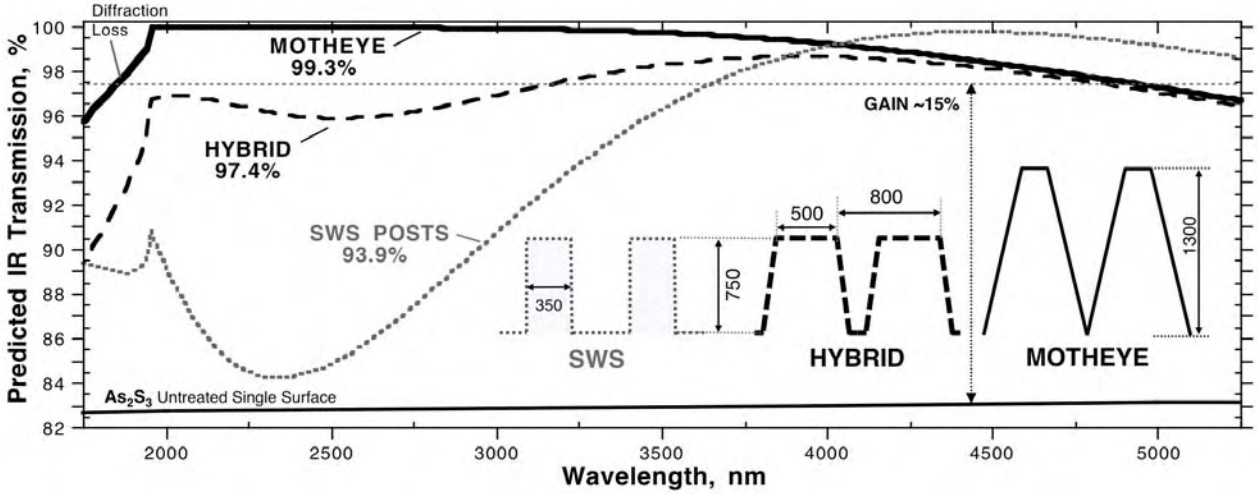

Figure 8: Predicted transmission of mid-IR light through various profile ARMs textures in As_2S_3.

In a direct embossing process, the molded material will have an ARMs structure that is the inverse or negative of the master, and this is the structure and material that must be modeled. For example, an ARMs master template with an array of tapered posts will print an array of tapered holes. A master with a symmetric profile design however, such as a square-grid array of pyramids, will result in an embossed structure that is similar to the master in profile and index grading. In addition to preliminary design functions, modeling is used to establish and characterize tradeoffs between desired optical performance and fabrication limitations. Manufacturing constraints and tolerances are intrinsic to molding and other replication processes. In replicating ARMs structures in moldable materials, performance and manufacturing collide; the widest bandwidth ARMs structures will have the highest aspect ratio, at the expense of a more difficult molding and release process. In addition, it is important to consider mass transport; a post-design master may mold a surface better than a hole-design master that might trap air and prevent full depth embossing. To evaluate the performance of hole-design Motheye structures embossed with a post-type master, a range of hole profiles was modeled in As_2S_3 for the CIRCM mid-IR spectral range. Figure 9 shows parabolic profile hole patterns on a square grid with varying duty cycle (hole diameter to hole spacing ratio) and depth. The models results indicate that larger duty cycles (dashed lines) have a greater impact on performance than hole depth, and that maximum performance over the laser tuning range can be obtained with little impact on the pump wavelength transmission.

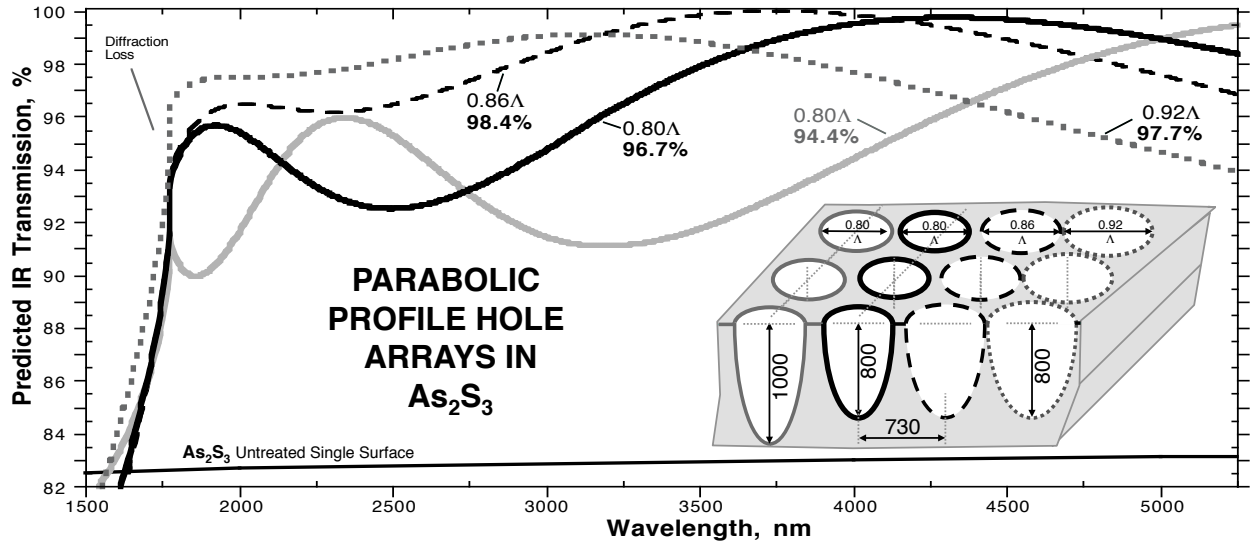

Figure 9: Predicted transmission of mid-IR light through graded-hole Motheye structures in As_2S_3.

5. MASTERING- MATERIALS and DESIGNS

For chalcogenide and related low glass transition temperature materials, the high performance benefit of ARMs technology can be achieved using an inexpensive and consistent replication process based on simple heat and pressure stamping, or embossing. The design and fabrication of master tooling is the most critical step in obtaining precise fidelity and high optical performance in the embossed material. Both Motheye and Hybrid ARMs designs have tapered structures, which can aid mass transport during embossing and minimizes resistance during mold release. Additional desirable master characteristics are manufacturability, high temperature stability, chemical compatibility for cleaning, mechanical durability, good thermal transport properties, and non-wetting properties during embossing. Optical transparency may also be beneficial for embossing schemes that include the ability to monitor the embossing sequence through the master substrate. Master molds designed for the CIRCM application have been produced in materials such as diamond, silicon carbide, sapphire, ALON, silicon, and nickel.

Fabrication into durable master materials is a two-step process that begins with the generation of a sacrificial mask pattern using an interference lithography process[23], followed by an etch process to transfer the pattern into the substrate. Traditional semiconductor industry etch processes tend to be either anisotropic (i.e. device processing) or isotropic (i.e. MEMs). For the SWS binary ARMs texture, an anisotropic etch is used to obtain vertical sidewall post or hole arrays. In contrast, both Motheye and Hybrid ARMs require precise control of etch rates of the substrate and mask materials. Etch processes have been developed for many materials that ablate the mask material during etching to effectively taper the structure and connect the bases, creating an optimal graded index profile.

Master Material Options: Polycrystalline diamond is an excellent choice for a master material due to its extreme durability, high thermal conductivity, and chemical resistance. An RIE etch process has been developed to produce diamond masters for CIRCM fiber embossing as illustrated by the SEM images in Figure 10.

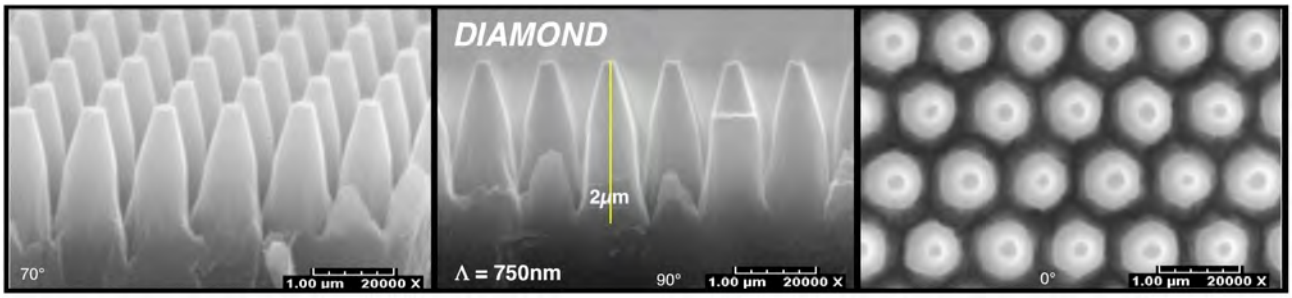

Figure 10: SEMs of an array of cones fabricated in the surface of a diamond window suitable for use as a stamping tool.

Sapphire and ceramics such as silicon carbide and ALON™ also have high thermal conductivity and similar mechanical and chemical durability as diamond. Figure 11 illustrates the type of rounded cone shapes built in silicon carbide that would produce the large duty cycle hole arrays needed for broad-band mid-IR transmission as with predicted by the models in Figure 9.

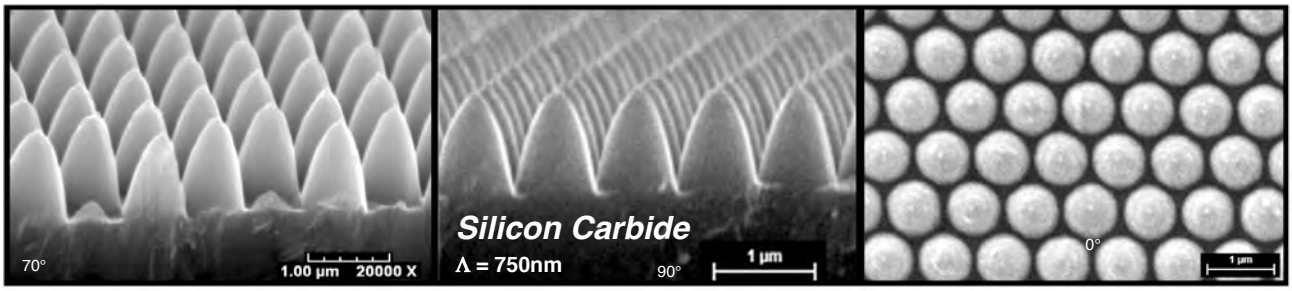

Figure 11: SEMs of an array of cones fabricated in the surface of a silicon carbide disc suitable for use as a stamping tool.

Master templates built in ALON and sapphire substrates are depicted in Figures 12 and 13. The visible light transparency of these materials permits in-situ replication validation through observation of changing interference and wetting effects during the heat and pressure application cycle.

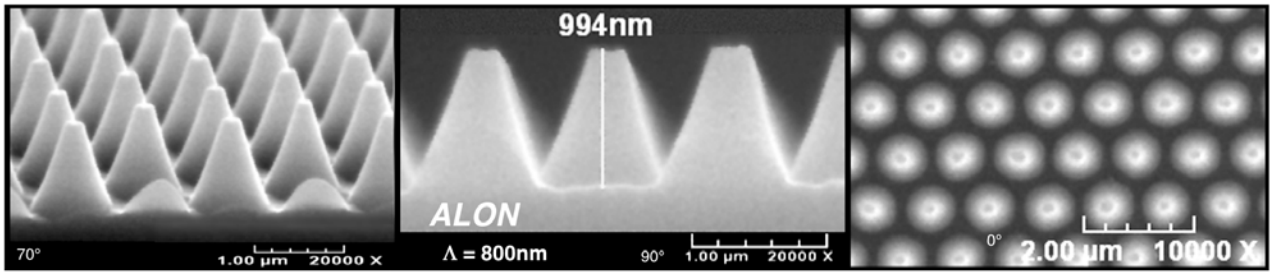

Figure 12: SEMs of an array of cones fabricated in the surface of an ALON substrate suitable for use as a stamping tool.

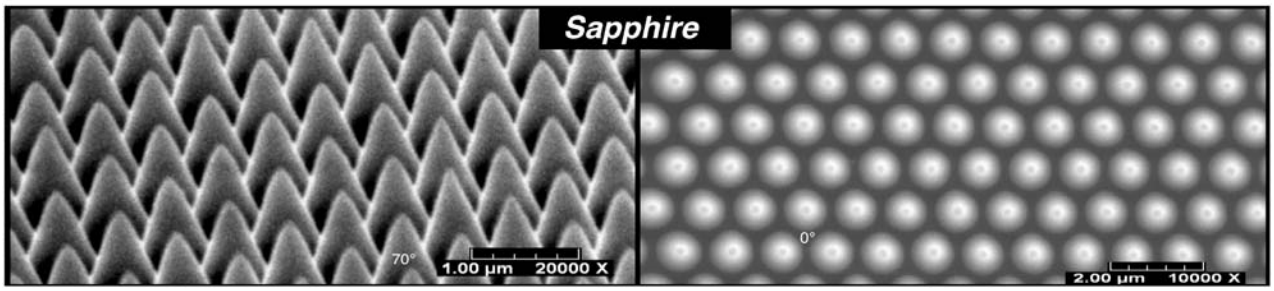

Figure 13: SEMs of an array of cones fabricated in the surface of a sapphire substrate suitable for use as a stamping tool.

Crystalline silicon lacks the mechanical durability of the diamond and ceramic masters, but ARMs textures with extreme and varied profiles can be produced readily. A silicon etch process has been optimized to yield deep tapered cone structures as depicted in Figure 14. The cones are about 2.3µm deep with a base dimension – or grid spacing – of just 0.8µm, The symmetry of the silicon pyramid array is also attractive for embossing since the replica will have the same profile as the master template.

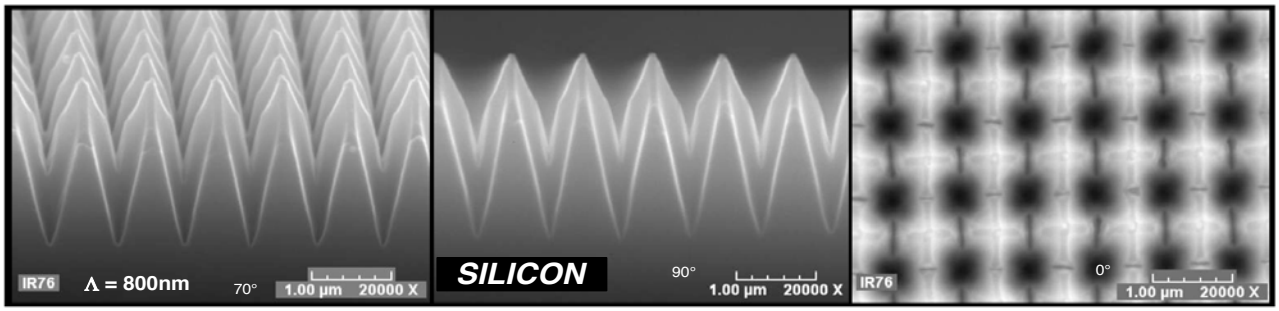

Figure 14: SEM images of a silicon master designed for broad-band mid-IR transmission when embossed in As_2S_3 fiber.

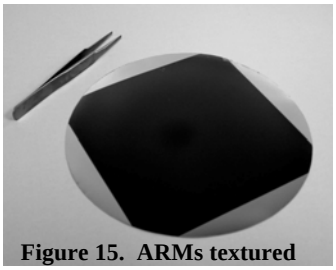

Figure 15. ARMs textured nickel electroform.

The compact disc and DVD industries rely on replicating products in high volume using hard, yet flexible nickel masters. Nickel templates have been produced for visible light ARMs textures intended for replication in plastic materials for applications such as display films and automotive instrument panel covers[26]. The nickel master fabrication sequence begins with interference lithography to define an ARMs texture original in a photoresist material coated on a glass carrier. The photoresist layer is then copied into the surface of a nickel plate through conventional electroforming processes to form a precise inverse or negative of the original pattern. Features in a final product embossed with the nickel shim will contain features exactly the same as the photoresist original. Figure 15 shows an image of a 200mm diameter nickel master produced by TelAztec for visible light display applications. In addition to the ease of fabrication, nickel master replicas can be made from a nickel original so that a particular pattern can be made into dozens of identical masters and used to effect high volume production. Figure 16 shows SEM images of a patterned photoresist layer on glass consisting of an array of parabolic profile holes that when converted into a nickel, would contain bullet shaped features. Pressings from this shim would take on the shape of the features in the original, yielding performance similar to the structures simulated in Figure 9.

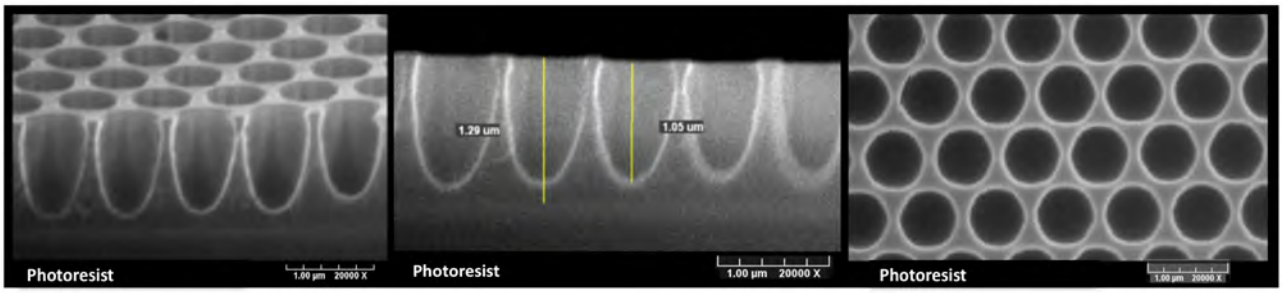

Figure 16: SEM images of a photoresist original used in the fabrication of a hard nickel stamping plate.

6. ARMs EMBOSSING TRIALS

Chalcogenide glasses by definition contain the elements sulfur, selenium or tellurium. Their glass transition temperature is low, typically less than 250C, allowing for softening and moldability using a variety of heat sources and configurations. As described above, chalcogenide materials are good candidates for CIRCM fiber optic beam delivery systems due to their mid IR transparency and recent improvements by researchers at NRL that have reduced its intrinsic absorption. IRPhotonics offers the fluoride glasses ZBLAN (ZrF4-BaF2-LaF3-AlF3-NaF) and indium fluoride (InF_3) as candidates for CIRCM and related IR fiber applications[27]. Both ZBLAN and InF_3 have low intrinsic loss and wide transparency from the UV to beyond 5µm, and a low index of refraction near 1.5 that results in lower reflection losses than chalcogenide materials. Glass transition temperature for these materials ranges from 260 to 320 C.

The definition of process parameters for replicating ARMs textures in fiber facets included embossing larger area surfaces so as to optimize parameters of force/area, temperature, pressure, and rate of pressure. NRL supplied several 1-inch round 2mm thick polished As_2S_3 windows for the embossing trials, and 20 AMTIR2 (As_2Se_3) 1-inch round by 3mm thick windows were purchased from Amorphous Materials Inc. For InF_3 and ZBLAN windows, IRPhotonics provided two small diameter cylindrical fiber optic pre-forms that were sliced into slabs and polished to yield multiple 8-10mm round, 1mm thick windows. Each of these materials was embossed using a simple apparatus to press a master template against a polished surface with controlled heat and pressure. In general, sticking issues between the master and embossed material were minimal. Trials where the embossed material exhibited damage correlated with excessive heat or pressure. Most of the substrates cracked due to thermal expansion mismatch and problems with mating two large area planar surfaces that would not be an issue with the rapid cycle times envisioned for the typical 200µm diameter fiber facets.

Initial embossing attempts in InF_3 substrates used diamond masters like that shown in Figure 10. The micro-textured diamond substrate was laser cut to 1.8 x 1.8mm die for use in the embossing apparatus. Good uniformity was seen in the embossed pattern as shown in Figure 17, however the 1µm depth attained is about half the depth of the diamond master features yielding a hole array duty cycle that is greatly reduced. The images suggest that the master template may have been released from the InF_3 material while it was still soft, leading to material re-flow. Similar re-flowed surfaces resulted from pressings using sapphire and silicon masters. In addition, pressing the 1.8mm square diamond template into the surface of the 8mm round InF_3 windows typically resulted in a stress point fracture where the finished pressing could not be tested for transmission. None of these issues is expected to be a problem when embossing fiber tips where the master template will be up to 50 times larger in area than the fiber facet.

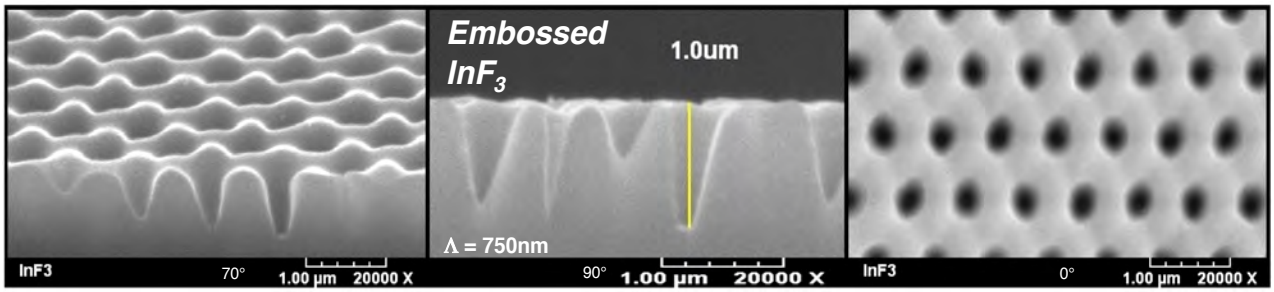

Figure 17: SEM images of ARMs textures embossed in the surface of an IRPhotonics InF_3 substrate.

The high aspect ratio silicon master shown in Figure 14 was used for ZBLAN embossing. Figure 18 shows the embossed structure with a clean high fidelity profile and 1.15µm depth. Note the interesting concave feature at the top of each post. This may be an indication of trapped air during the embossing cycle that may have limited the depth of the pressing. With the sharp valley features, there does not appear to be the re-flow issue upon release found with the InF_3 material and using this combination of silicon master and replica material.

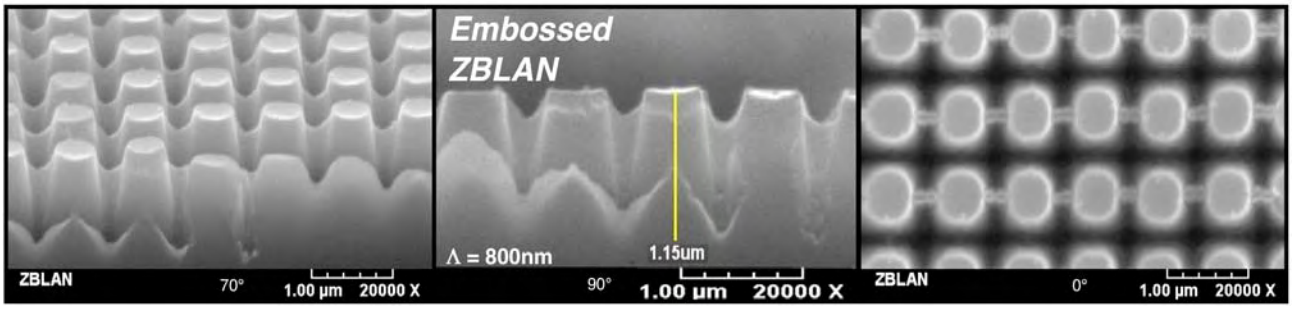

Figure 18: SEM images of ARMs textures embossed in the surface of an IRPhotonics ZBLAN substrate.

The Figure 14 silicon master was also used for embossing the NRL As_2S_3 coupons. Much of this development work was spent on optimizing the embossing parameters for As_2S_3 material in order to yield a large enough pressing area to for a spectral transmission measurement that could be compared to the wide bandwidth transmission increase seen with directly etched ARMs textured As_2S_3 windows. Fortunately, the As_2S_3 material proved to be readily moldable at low temperatures and pressures yielding exceptionally uniform and smooth structures as can be seen in Figure 19. A classic Motheye texture was produced with pyramidal post features 1.75µm deep and a profile matching the silicon master.

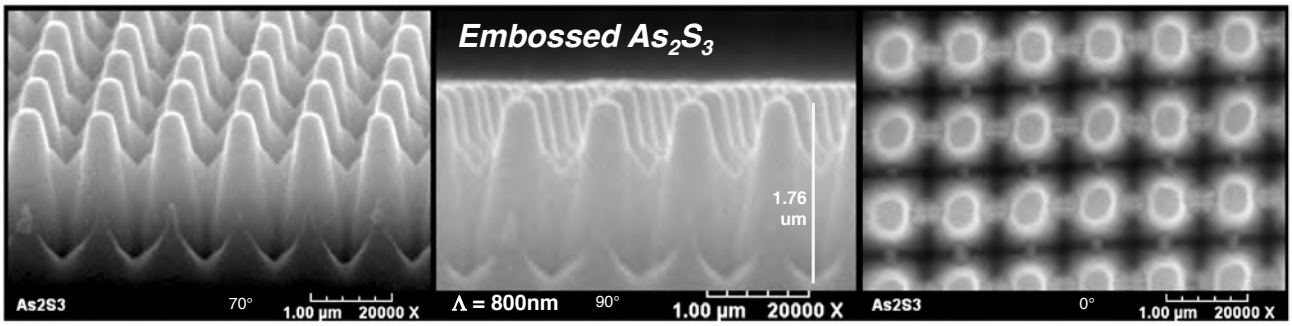

Figure 19: SEM images of ARMs textures embossed in the surface of an NRL As_2S_3 substrate.

The Figure 19 replica area was sufficient to make a spectral transmission measurement using the Nicolet FTIR spectrometer. From the refractive index data for As_2S_3 provided by NRL, the measured transmission of the embossed ARMs replica was normalized to the 83% single surface transmission expected, and plotted in comparison to the transmission of an As_2S_3 window fabricated with ARMs textures using the lithography and etch processes. Figure 20 shows the normalized transmission data taken over the mid-IR spectral range of 1.8µm to 6.0µm, where the data from the embossed replica is depicted as the solid black curve, and the data for the etched ARMs textured sample is shown as the solid gray curve. Both the embossed and etched samples have comparable transmission at 2.1µm with the embossed sample exhibiting less than 1% reflection loss. The embossed sample also shows a sharper diffraction edge, defined as the wavelength below which transmission loss is due to propagating free-space diffracted energy, that is the result of the smoother features producing less scattered light. These factors indicate that an equally high laser damage threshold will be found for embossed ARMs textures as that found for the etched ARMs textures (Figure 7). Overhead view SEM images of the etched (right) and embossed (left) ARMs textures are shown as an inset to the figure. The flat top profile combined with the shorter cone height (1.15µm embossed, 1.5µm etched) likely explains the longer wave fall off of the embossed texture relative to the etched texture. Both textured samples exhibit an exceptionally wide bandwidth with the embossed sample exhibiting less than 2.5% average reflection loss over the entire mid-IR band from 2.0-5.0µm.

As_2Se_3 glass, sold as AMTIR2 by Amorphous Materials, has a long wave infrared transparency that extends out to 14µm. CorActive sells an As_2Se_3 based multi-mode fiber with an absorption level that permits many meter length fibers to transmit well out to a wavelength of 10µm. The capability of ARMs technology to suppress light reflections

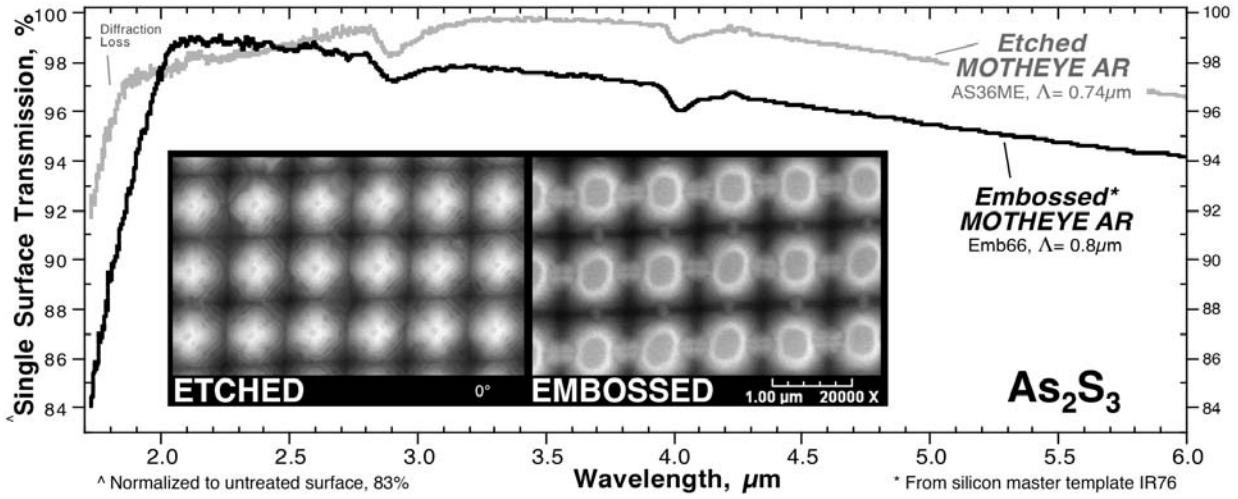

Figure 20: Normalized transmission data for embossed As_2S_3 substrate

over the increased bandwidth provided by As_2Se_3 glass was investigated through additional embossing trials. Several AMTIR2 substrates were stamped using the high aspect ratio Figure 14 silicon master where if the 2μm feature depth could be replicated uniformly in the AMTIR2 substrate surface, a transmission enhancement could be expected to extend over both the mid-IR (2-5μm) and long wave IR (LWIR 8-12μm). Initial tests used a 1-inch square silicon template to completely cover the surface of the 1-inch round AMTIR2 substrates. This configuration produced highly non-uniform pressings where only the high points making initial contact during the embossing cycle yielded full depth textures. Small area masters just large enough to yield sufficient area to be measured in the FTIR system had a further problem of creating stress points that would crack the AMTIR2 substrates during temperature cycling or master release. An intermediate silicon master size of about 15mm square worked best with the AMTIR2 and silicon master clamped between sapphire optical flats. Fracturing and non-uniformity were still a problem but many sections were large enough to obtain transmission measurements as shown in Figure 21. A transmission increase over an untreated window (solid black line) of from 6 to 11% is found for one section (solid gray line) over the huge infrared wavelength range of from 2 to 12μm. A more typical transmission increase of from 4 to 10% over the same wavelength range was measured for areas near the center of the pressing (dashed black line). With improved fidelity embossing methods that yield fewer pattern defects, the maximum 15% transmission increase could be attained over the entire 2 to 12μm range.

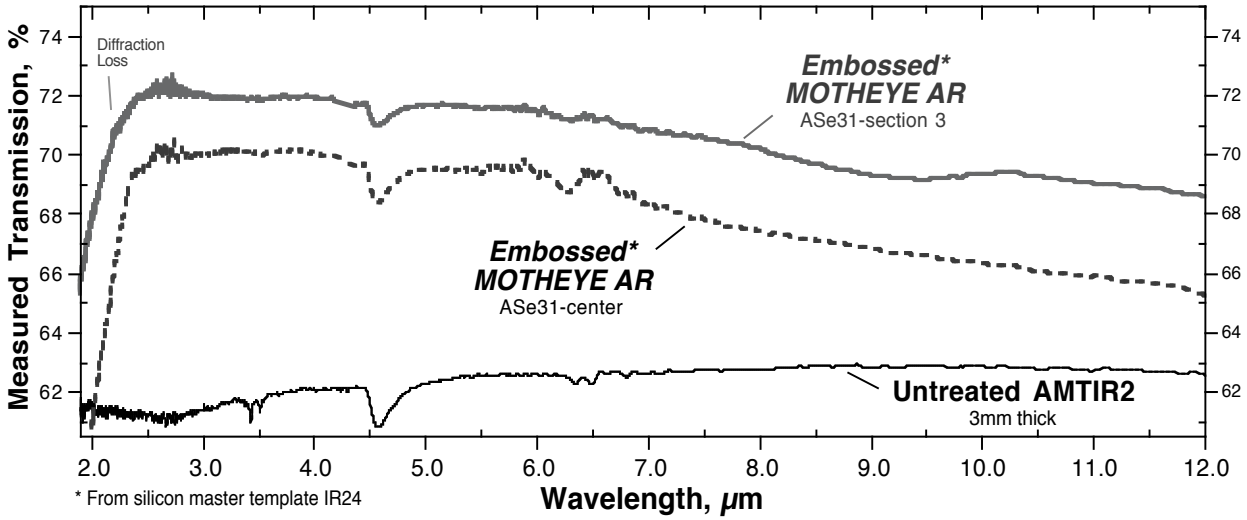

Figure 21: Ultra-wide band IR transmission enhancement of AMTIR2 windows embossed with ARMs textures in 1 surface.

7. CHALCOGENIDE FIBER EMBOSSING

CorActive provided several meters of their bare As_2S_3 multimode fiber with a 100µm diameter core, 35µm thick cladding, for use in ARMs embossing trials. In addition, Daylight Solutions Inc., a major supplier of mid-IR lasers and components, provided many stub length As_2S_3 fibers with custom high power laser terminations to be used for establishing a path toward applying ARMs textures to fibers in fully assembled cable systems. Figure 22 on the right shows an As_2S_3 fiber protruding from the center of a cylindrical ferule that forms part of an Amphenol SMA type 905 stainless steel fiber termination. The ferule has a recessed well at the end that may be useful for preventing fiber tip damage when connected to a high power laser system.

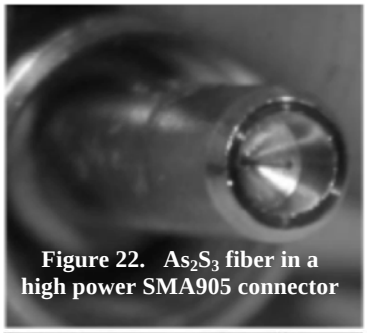

Figure 22. As_2S_3 fiber in a high power SMA905 connector

A bench top fiber embossing tool was assembled with independent control of temperature, pressure, and contact time. Aligning the fiber facet and master template surfaces was achieved using off-the-shelf translation and angle manipulators with 5 independent axes controlled by manual micrometers. Bare test fibers were first inserted in SMA905 connectors so that the end facets had a slight extension beyond the connector ferrule that facilitated polishing. Overhead, elevation and profile views of this fiber termination are shown in the SEM images on the right The protruding facet configuration allowed for embossing the fiber tip with large area master templates, and yielded slightly convex surfaces after polishing that is believed to be preferable for embossing. The embossing temperature was considerably above the glass transition temperature (Tg) of As_2S_3, using process parameters determined during the substrate embossing effort.

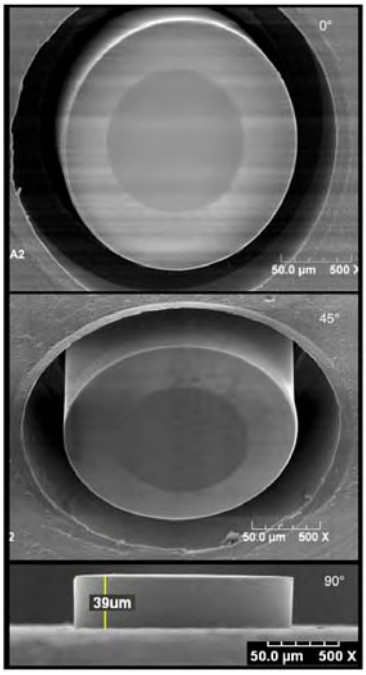

Initial development work was completed with sacrificial fiber ferrule stubs to further optimize process parameters, and to permit evaluation of the embossed structures in SEM. The pyramidal structure ALON master shown in Figure 12 was used. Figure 23 shows SEM images of the embossed profile of 2 fiber tips. It is believed that both fibers exhibit full depth ARMs profiles across the fiber cores, as the texture appears to be the inverse of the master profile, notably the width of the openings correspond to base size on the ALON master. The upper fiber has full printing across the 100µm core, but limited printing in the cladding area. The lower fiber shows full embossing out to the fiber edge, with a small degree of compression of the fiber tip. The prototype embossing effort demonstrates the fidelity and precision that can be attained with the ARMs treatment approach for fibers. Failure mechanisms identified with the fiber embossing trials are as expected, either overheating or over compressing the fiber tip, which can be eliminated with additional process development and system automation with dynamic feedback monitoring.

A secondary advantage of the embossing process is the ability to rework or re-mold fiber ends if desired; directly embossing over an existing print, or by planarizing the tip surface with a blank master and then re-molding. Re-embossing fiber tips has been performed many times, with no relic of previous texture when full depth is attained in the final embossing. This should enable a low cost process for fiber facet restoration in the event of mechanical or power handling damage to the expensive optical cable assembly.

Measuring the mid-IR spectral transmission through optical fiber using a conventional FTIR equipped with a simple resistively heated infrared light source is proving to be a major challenge. A commercially available FTIR fiber analysis accessory was evaluated using untreated and embossed fibers. Very little light could be coupled into the fibers using the accessory, resulting in excessively noise in the recorded signal. Despite this difficulty, transmission measurements of As_2S_3 fibers before and after ARMs embossing showed a 5 to 10% transmission enhancement, but with an uncertainty of at least 5% due to the low signal level and high noise level. A custom test jig is being assembled that will significantly improve the fiber coupling efficiency in the FTIR spectrometer that will allow for fiber embossing and in-situ transmission testing. Single wavelength laser transmission testing is also planned as future work, for the dual purpose of transmission measurement and power transmission capacity and long term reliability testing.

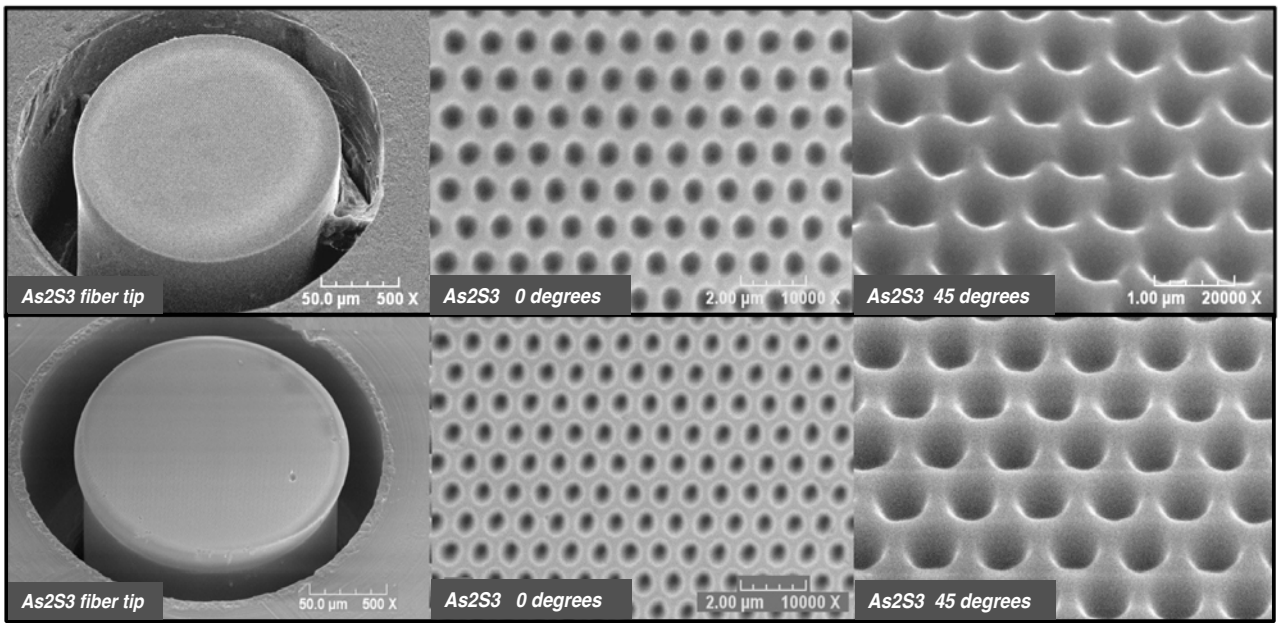

Figure 23: SEM images of two fiber tips uniformly embossed with ARMs textures.

Scheduled improvements to the embossing tool will include the capability to emboss fiber facets that are recessed below the connector ferule surface using precision cut and aligned masters. The embossing process itself will be automated with visual feedback through transparent replication masters such as sapphire and diamond, to monitor interference fringes and optical contact or "wetting" during pattern transfer. The application of ARMs textures in fibers that are fully assembled into cables will be offered as a commercial service.

8. SUMMARY

AR microstructure technology continues to show great potential for yielding high performance optics with enhanced durability in high power laser systems. This study demonstrated the feasibility of replicating ARMs textures in the chalcogenide and fluoride glasses of optical fiber beam delivery systems envisioned for CIRCM anti-missile systems and related high power laser applications. New laser damage test results for ZGP and GaAs laser materials that supplement previous findings in As_2S_3 and CZT, demonstrate that ARMs textures are significantly more durable than multi-layer thin film AR coatings. Optical performance modeling was presented to guide the design of master stamping tools in several durable materials. ARMs textures embossed in As_2S_3 and As_2Se_3 materials, and the fluoride glasses InF_3 and ZBLAN, show excellent pattern transfer and fidelity. Transmission data from large area replicas show broadband mid-IR optical performance equivalent to directly fabricated ARMs textures along with the potential for extremely wide band performance extending into the LWIR. Preliminary trials of the direct molding of high performance ARMs into the end facets of As_2S_3 fiber optic cables has yielded promising initial results.

9. ACKNOWLEDGEMENTS

The authors thank Michael Thomas of SPICA Technologies who provided the difficult and hazardous laser damage testing of the chalcogenide materials presented, as well as the damage testing of the ZGP and GaAs materials. Terminated and polished As_2S_3 fiber stubs along with fully assembled cables were provided by Daylight Solutions (DLS). As_2S_3 substrates for the embossing development work were provided courtesy of the Naval Research Laboratories (NRL). CorActive provided As_2S_3 fiber for fiber embossing development work. The ZBLAN and InF_3 materials were supplied by IRPhotonics. All SEM analysis was performed by Mr. John Knowles at MicroVision Laboratories, Inc., (978-250-9909).

10. REFERENCES

[1] Fulghum, D.A., “Countermeasures Capabilities Become Clearer”, Aviation Week, 19 JAN (2010)
[2] Fulghum, D.A., “Defeating IR Missiles”, Aviation Week, Special Report: Electronic Warfare, 15 JAN (2010)
[3] Warwick, G., “RFP For U.S. Army Laser Jammer Expected Soon”, Aviation Week, 29 SEPT (2010)
[4] Aggarwal, I.D., and Sanghera, J.S., “Development and applications of chalcogenide optical fibers at NRL”, J. Optolectronics and Advanced Materials, **4**, 3, (2002).
[5] Sanghera, J.S., et. al., “Reduced Fresnel losses in chalcogenide fibers by using anti-reflective surface structures on fiber end faces”, Optics Express **18**, 25, (2010).
[6] Curatua, G., et. al., “Using molded chalcogenide glass technology to reduce cost in a compact wide-angle thermal imaging lens”, Proc. SPIE **6206**, (2006).
[7] Curatua, G., “Design and fabrication of low-cost thermal imaging optics using precision chalcogenide glass molding”, Proc. SPIE **7060**, (2008).
[8] Bordé, P., et. al., “Updated results on prototype chalcogenide fibers for 10 μm wavefront spatial filtering”, Proc. of the Conference on Other Earths: DARWIN/TPF and the Search for Extrasolar Terrestrial Planets, 371, (2003).
[9] Sanghera, J.S., personal communication and announced during the Window and Dome session, 28 April (2011)
[10] Testing results by personal communication from Dr. John Whikman, BAE Systems, (2009)
[11] Lowdermilk, W.H. and Milam, D., “Graded-index antireflection surfaces for high-power laser applications”, Appl. Physics Letters, **36** (11), 891 (1980).
[12] Hobbs, D.S., MacLeod, B.D., “High Laser Damage Threshold Surface Relief Micro-Structures for Anti-Reflection Applications”, Proc. SPIE **6720**, 67200L (2007).
[13] Bernhard, C. G., "Structural and functional adaptation in a visual system", Endeavour, **26**, 79 (1967).
[14] Clapham, P.B., Hutley, M.C., "Reduction of lens reflexion by the 'Moth Eye' principle", Nature, **244**, 281 (1973).
[15] Wilson, S.J., Hutley, M.C., "The optical properties of 'moth eye' antireflection surfaces", Optica Acta, **29** 7 (1982)
[16] Southwell, W. H., "Pyramid-array surface-relief structures producing antireflection index matching on optical surfaces", JOSA A, **8** (3), 549 (1991).
[17] Raguin, D.H., and Morris, G.M., "Antireflection structured surfaces for the infrared spectral region", Appl. Optics, **32** (1993).
[18] Hobbs, D.S., MacLeod, B.D., “Design, Fabrication and Measured Performance of Anti-Reflecting Surface Textures in Infrared Transmitting Materials”, Proc. SPIE **5786**, (2005).
[19] Hobbs, D.S., MacLeod, B.D., “Update on the Development of High Performance Anti-Reflecting Surface Relief Micro-Structures”, Proc. SPIE **6545**, 65450Y (2007).
[20] MacLeod, B.D., Hobbs, D.S., “Long Life, High Performance Anti-Reflection Treatment for HgCdTe Infrared Focal Plane Arrays”, Proc. SPIE **6940**, 69400Y (2008).
[21] Hobbs, D.S., et. al., “Performance of HgCdTe IR FPAs Incorporating Microstructure-Based AR Treatments (U)”, Military Sensing Symposia, **MSS2009**, (2009).
[22] Hobbs, D.S., “Study of the Environmental and Optical Durability of AR Microstructures in Sapphire, ALON, and Diamond”, Proc. SPIE **7302**, 73020J (2009).
[23] Hobbs, D.S., et. al., “Automated Interference Lithography Systems for Generation of Sub-Micron Feature Size Patterns”, Proc. SPIE **3879**, 124 (1999).
[24] Zawilski, K.T. et al, “Large aperture single crystal $ZnGeP_2$ for high-energy applications”, J. Crystal Growth, **310**, 7, (2008)
[25] Zawilski, K.T. et al, “Laser damage threshold of single crystal $ZnGeP_2$ at 2.05 μm”, Proc. SPIE, **5991**, (2005).
[26] MacLeod, B.D., Hobbs, D.S., “Low-Cost Anti-Reflection Technology For Automobile Displays”, J. SID, (2004).
[27] Poulain, M., “Fluoride glass fibers: applications and prospects”, Proc. SPIE **3416**, 2 (1998)
[28] Hobbs, D.S., “Laser damage threshold measurements of anti-reflection microstructures operating in the near UV and mid-infrared”, Proc. SPIE **7842**, 78421Z (2010)